

## Results on the disconnected contributions for hadron structure

---

### Constantia Alexandrou

*Department of Physics, University of Cyprus, P.O. Box 20537, 1678 Nicosia, Cyprus  
Computation-based Science and Technology Research Center, Cyprus Institute, 20 Kavafi Str.,  
Nicosia 2121, Cyprus  
E-mail: alexand@ucy.ac.cy*

### Martha Constantinou

*Department of Physics, University of Cyprus, P.O. Box 20537, 1678 Nicosia, Cyprus  
E-mail: marthac@ucy.ac.cy*

### Vincent Drach

*CP3 Origins & DIAS, University of Southern Denmark, Campusvej 55, DK-5230 Odense M,  
Denmark  
E-mail: drach@cp3.dias.sdu.dk*

### Kyriakos Hadjiyiannakou

*Department of Physics, University of Cyprus, P.O. Box 20537, 1678 Nicosia, Cyprus  
E-mail: ph07hk2@ucy.ac.cy*

### Karl Jansen

*NIC, DESY, Platanenallee 6, D-15738 Zeuthen, Germany  
E-mail: Karl.Jansen@desy.de*

### Giannis Koutsou

*Computation-based Science and Technology Research Center, Cyprus Institute, 20 Kavafi Str.,  
Nicosia 2121, Cyprus  
E-mail: g.koutsou@cyi.ac.cy*

### Alejandro Vaquero\*

*Computation-based Science and Technology Research Center, Cyprus Institute, 20 Kavafi Str.,  
Nicosia 2121, Cyprus  
E-mail: a.vaquero@cyi.ac.cy<sup>†</sup>*

We present results on the disconnected contributions to three point functions entering in studies of hadron structure. We use  $N_f = 2 + 1 + 1$  twisted mass fermions and give a detailed description on the results of the nucleon sigma-terms, isoscalar axial charge and first moments of bare parton distributions for a range of pions masses. In addition we give the  $\sigma$ -terms and the computations are performed using QUDA code implemented on GPUs.

*The 32nd International Symposium on Lattice Field Theory,  
23-28 June, 2014  
Columbia University New York, NY*

---

\*Speaker.

<sup>†</sup>Present address: Alejandro.Vaquero@mib.infn.it, INFN Sezione Milano Bicocca.

## 1. Introduction

Most studies of hadron structure have neglected the disconnected quark loop contributions due to the technical difficulty associated with the computation of these diagrams. Algorithmic developments as well as new computer architectures are making the computation of disconnected contributions feasible and enable us to reach the high precision necessary for obtaining meaningful results on these quantities. In this work we employ GPUs for the complete evaluation of the disconnected quark loops that contribute to the nucleon observables [1]. Our implementation on GPUs includes the inversion of the Dirac operator, contractions and Fourier transform. To this end we make extensive use of the QUDA library [2].

## 2. Variance reduction techniques

The basic quantity that enters in the computation of disconnected quark loops is the trace of the inverse of the fermionic matrix. Since a direct computation is unaffordable, stochastic techniques are used (recently an alternative approach was developed based on hierarchical probing [3, 4]), to estimate the inverse matrix by employing stochastic noise sources<sup>1</sup>. But stochastic techniques have inherent noise that decreases as  $O(1/\sqrt{N_r})$ , with  $N_r$  the number of stochastic sources employed. In addition, disconnected quark loops are prone to large gauge noise and therefore variance reduction techniques are essential to obtain a good signal.

### 2.1 The Truncated Solver Method

In this work we employ the well known Truncated Solver Method (TSM) [6] that is found to be well-suited in disconnected diagram computations due to its effectiveness and its low cost. The basics of the TSM consist of computing a cheap, low-precision estimation of the inverse matrix by truncating the inverter using many stochastic noise sources, and then correcting it by a few high-precision inversions. The correction is estimated by inverting a few noise sources to both high- and low-precision, and averaging over the difference as follows

$$M_{E_{TSM}}^{-1} := \frac{1}{N_{HP}} \sum_{r=1}^{N_{HP}} [|s_r\rangle_{HP} - |s_r\rangle_{LP}] \langle \eta_r | + \frac{1}{N_{LP}} \sum_{j=N_{HP}}^{N_{HP}+N_{LP}} |s_r\rangle_{LP} \langle \eta_r | x. \quad (2.1)$$

If the high- and the low-precision inversions yield results that are highly correlated, the correction does not fluctuate excessively, and a few sources are enough to correct the bias. One then can use computer resources to increase the number of the low-precision estimators, reducing the statistical error cheaply.

### 2.2 The one-end trick

The twisted-mass fermion regularization scheme (tmQCD) has a unique feature that allows for the use of a very powerful variance reduction technique for the disconnected contributions [7]. By using the identities

<sup>1</sup>In this work we use  $Z_N$  noise, as it was reported to be optimal [5].

$$M_u^{-1} - M_d^{-1} = -2i\mu a M_d^{-1} \gamma_5 M_u^{-1}, \quad (2.2)$$

$$M_u^{-1} + M_d^{-1} = 2D_W, \quad (2.3)$$

any computation featuring a sum/difference of propagators is automatically improved. Note that we only need to replace the fields in the contraction by

$$\frac{2i\mu a}{N_r} \sum_{r=1}^{N_r} \langle s_r^\dagger \gamma_5 X s_r \rangle = \text{Tr}(M_u^{-1} X) - \text{Tr}(M_d^{-1} X) + O\left(\frac{1}{\sqrt{N_r}}\right), \quad (2.4)$$

$$\frac{2}{N_r} \sum_{r=1}^{N_r} \langle s_r^\dagger \gamma_5 X \gamma_5 D_W s_r \rangle = \text{Tr}(M_u^{-1} X) + \text{Tr}(M_d^{-1} X) + O\left(\frac{1}{\sqrt{N_r}}\right). \quad (2.5)$$

This trick reduces the signal-to-noise ratio of the computation from  $O\left(\frac{1}{\sqrt{V}}\right)$  to  $O(1)$ .

### 3. GPU acceleration

The QUDA library is used throughout for these calculations with the exception of the generation of the sources, that is carried out on CPUs. Once the source is copied to the GPU, the rest of the computations are performed there. Taking advantage of the specific capabilities of the GPUs, the high-precision correction was computed using a mixed double-single precision solver, performing at  $\approx 100$  GFlops per GPU, whereas the low-precision estimation used a mixed double-half precision solver, yielding the impressive amount of  $\approx 300$  GFlops per card. The contraction kernels in double precision achieve a performance of around 300 GFlops, solving one of the most important bottlenecks that slowed down the loop computations on GPUs for some time. These kernels, developed by our group [8], deliver results for all possible  $\gamma$  insertions for ultra-local and one-derivative operators, which allowed us to perform a complete analysis of all disconnected loop contributions to hadron structure. The Fourier transform required was performed by employing the highly optimized CUDA library cuFFT. These improvements enable a very efficient computation of the disconnected quark loops.

### 4. Ensembles

We show results for two different tmQCD  $N_F = 2 + 1 + 1$  ensembles:

Ensemble	Volume	$m_\pi$ (MeV)	$m_\pi L$	$a$ (fm)	Stats
B55.32	$32^3 \times 64$	372(5)	4.97	0.0823(10)	147072
D15.48	$48^3 \times 96$	213(21)	3.35	0.0646(7)	7752

**Table 1:** Ensembles used in the calculation.

Both the strange and the charm quark masses were tuned to their physical values for both ensembles. The low-precision inversions used a residual of  $\rho \approx 5 \times 10^{-3}$ , while the high-precision

inversion used  $\rho \approx 10^{-9}$ . For the D15.48 ensemble we computed 24 high-precision propagators for the correction and 500 low-precision ones for the estimation for all flavors. For the B55.32 we also use 24 high-precision propagators and 500 low-precision ones for the light quark sector, while for the strange and the charm quark sectors 300 low-precision propagators are used.

## 5. Results on nucleon observables

We show results on the bare nucleon  $\sigma$ -terms in Fig. 1 that describe the scalar content of the nucleon, and are highly relevant in dark matter searches. Comparing the results of both ensembles we appreciate a clear decrease in the importance of the contribution of  $\sigma_{\pi N}$  disconnected, whereas  $\sigma_s$  grows with diminishing mass. The behavior of  $\sigma_c$  with the pion mass is not clear to us, for from the data coming from the B55 ensemble we couldn't find a reasonable value.

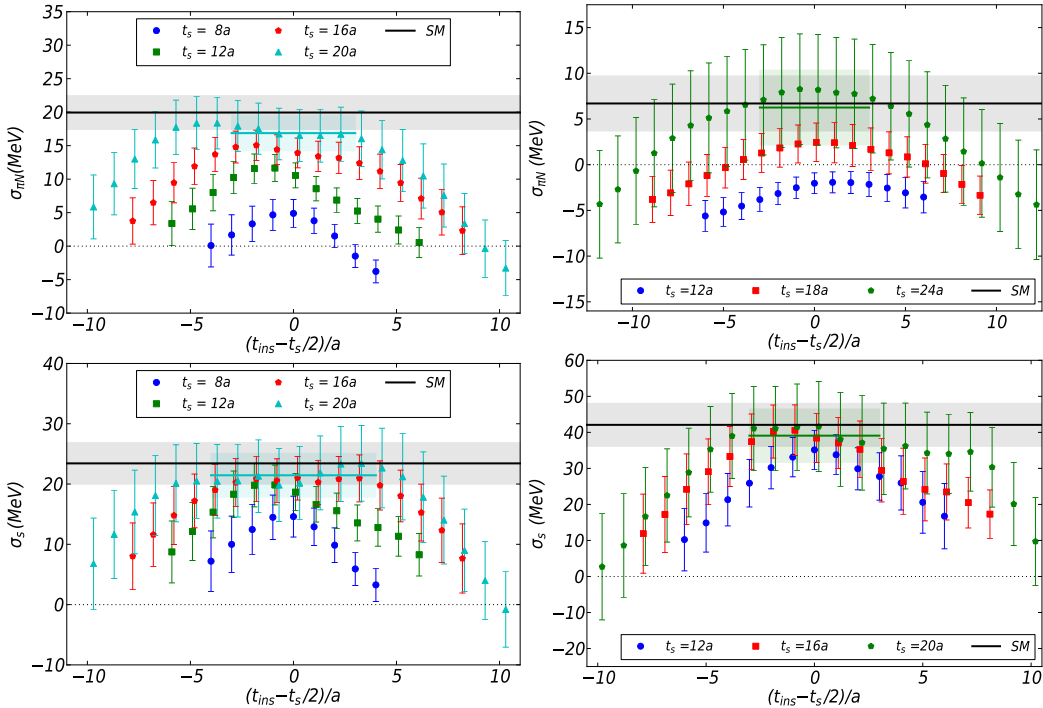


**Figure 1:** Plateau method for the nucleon  $\sigma_{\pi N}$  (upper panel) and  $\sigma_s$  (lower panel) for the B55.32 (left) and D15.48 (right) ensembles. Contamination from excited states is evident, as the value of the plateau increases with increasing  $t_s$  up to  $t_s \sim 1.5$  fm. The grey band is the result obtained from the summation method.

Using these two ensembles and a linear extrapolation in  $m_\pi^2$  we find (for the disconnected, no connected contributions here)  $\sigma_{\pi N} = 3.9 \pm 4.5$  MeV and  $\sigma_s = 47.8 \pm 8.7$  MeV at the physical point. Given that we only have two ensembles, with limited statistics for the D15.48, the values of the  $\sigma$ -terms quoted are to be regarded as preliminary. The important point is that we have a method that with increased statistics can be applied to the computation of these important observables.

The value of the axial charge  $g_A^q$  determines the intrinsic fraction of the spin carried by a quark  $q$  in the proton. Given the long-standing spin puzzle of the nucleon it is important to be able to compute this quantity directly from QCD. To extract  $g_A^q$  we need both the isovector and isoscalar values of the matrix element of the axial-vector current. In Fig. 2 we show the results

on the disconnected part of the isoscalar<sup>2</sup>  $g_A^{u+d}$  and strange contribution to the spin  $g_A^s$ . If one

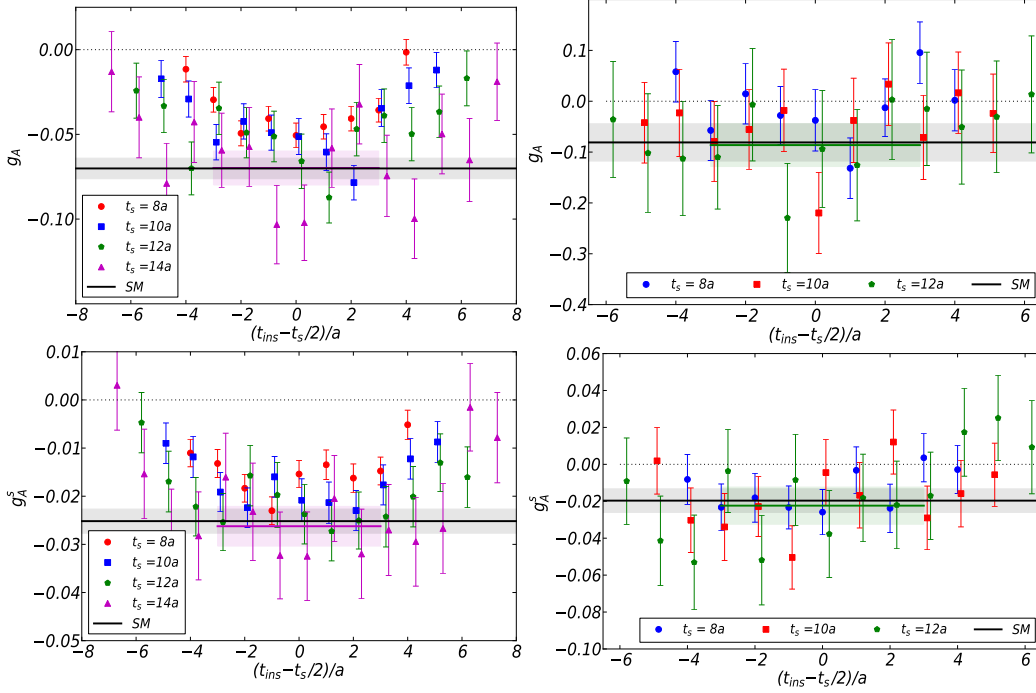


**Figure 2:** Plateau method for the bare nucleon  $g_A^{u+d}$  (upper panel) and  $g_A^s$  (lower panel) for the B55.32 (left) and D15.48 (right) ensembles. No noticeable contamination from excited states is observed.

extrapolates to the physical pion mass to LO (constant fit), one obtains  $g_A^{u+d} = -0.075 \pm 0.038$  and  $g_A^s = -0.0212 \pm 0.0072$ . While these numbers are preliminary it is clear that the correction to the connected part is  $\approx 10\%$ , and therefore disconnected contributions must be taken into account in determining high precision results for the spin content of the nucleon.

Our study includes loops with all  $\gamma$ -structure and thus also the tensor combination entering in the tensor content of the nucleon. Contrary to  $g_A^{u+d}$  our results on  $g_T^{u+d}$  displayed in Fig. 3 show that the disconnected contribution is very small and can be neglected compared to the connected contribution. This is also true for  $g_T^s$ .

Our results include disconnected contributions entering the momentum fraction carried by the light and the strange quarks in the nucleon. Within our accuracy these are found consistent with zero for the B55.32 ensemble as shown in Fig. 4 for the momentum fraction and helicity. Similar results are obtained for the D15.48 ensemble.

## 6. The physical point

In order to eliminate the systematic error due to the chiral extrapolation one needs to compute the disconnected contributions directly at the physical point. Although we have an ensemble of twisted mass fermion with a clover term at the physical point, applying the methodology developed

<sup>2</sup>For the renormalization we use the isovector  $Z_A$ . The error introduced is of order  $O(g_0^2)$ , much smaller than our current statistical errors.

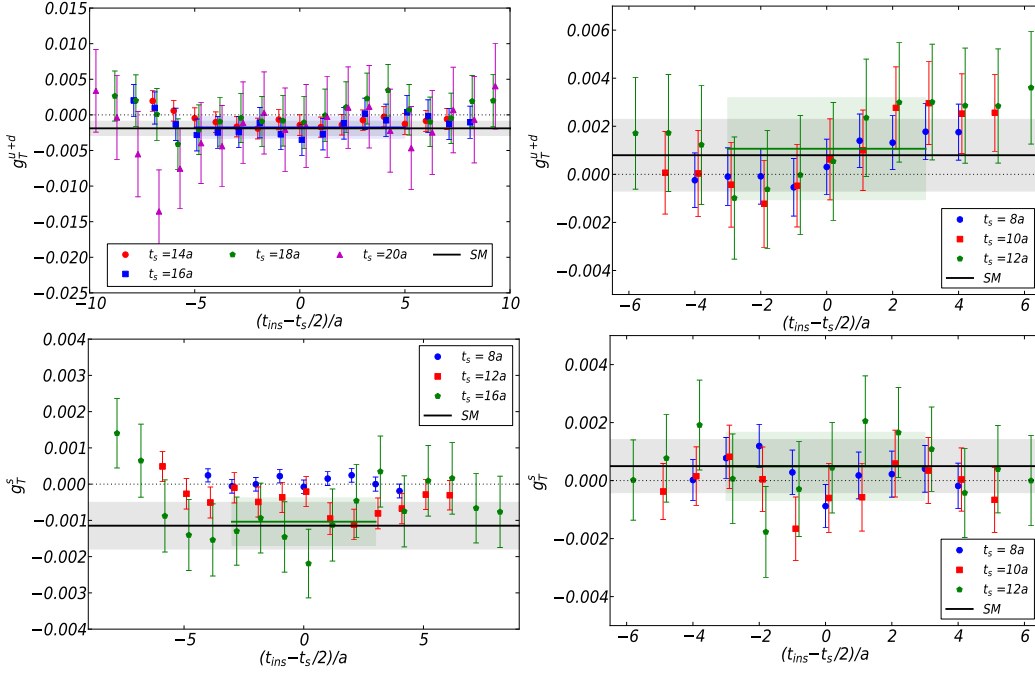


**Figure 3:** Plateaux for  $g_T^{u+d}$  (upper panel) and  $g_T^s$  (lower panel) of the nucleon for the B55.32 (left) and the D15.48 (right) ensembles.

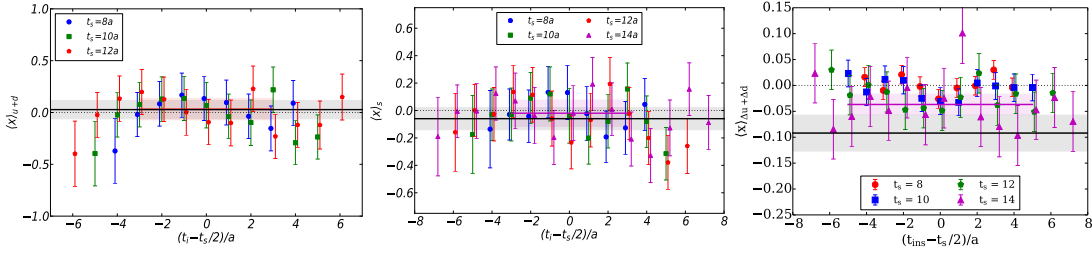


**Figure 4:** Results for  $\langle x \rangle_{u+d}$  (left),  $\langle x \rangle_s$  (center) and  $\langle x \rangle_{\Delta u + \Delta d}$  (right) of the nucleon for the B55.32 ensemble.

for larger pion masses proved to be insufficient. The reason is that the size of the correction involved in the TSM algorithm grows as the mass decreases, requiring a large number of high-precision inversions (and hence becoming prohibitively expensive) to obtain a reliable value for the quark loops. Reducing the residual of the low-precision estimation can help, but increases the cost of the computation up to a level that the TSM is not efficient any more. Attempts to tune for the best values following the procedure outlined in [6] failed to give parameters that would make the TSM competitive so far. Since the low-modes of the Dirac operator are expected to be responsible for this behavior, we are exploring deflation techniques in order to remove them. There already exists reports on the performance of the deflated TSM, usually called Truncated Eigenmode Acceleration (TEA) [11].

## 7. Conclusions

The disconnected contributions are becoming finally accesible by a clever combination of computer power and state-of-the-art algorithms. This allowed us to carry out a broad, high-

precision study that included all the possible disconnected contributions with ultra-local and one-derivative insertions. The final objective is to remove the systematic errors that appear in many hadron structure studies, as well as calculate all these disconnected contributions that have interest by themselves (e.g.  $\sigma_s$  for dark matter searches) to a new level of precision.

In spite of the large improvements recently made in algorithms, high statistics are still required to obtain good signal in many observables. The most accurate results presented here were for  $\approx 150000$  measurements, and even at such high statistics we were not able to achieve the accuracy typically achieved with connected contributions for all observables.

In the future we plan to deliver data obtained directly at the physical pion mass. To this end we will include deflation in our code and calculate the low-modes exactly.

## 8. Acknowledgements

A. Vaquero and M. Constantinou are supported by the Cyprus Research Promotion Foundation (RPF) under contracts EPYAN/0506/08 and TECHNOLOGY/ΘΕΠΠΣ/0311(BE)/16 respectively and K. Jansen partly by the RPF project ΠΡΟΣΕΛΚΥΣΗ/ΕΜΠΕΙΡΟΣ/0311/16. This work was partly funded by the RPF project ΝΕΑΥΠΙΟΔΟΜΗ/ΣΤΡΑΤΗ/0308/31 (infrastructure project Cy-Tera, co-funded by the European Regional Development Fund and the Republic of Cyprus through the RPF). Computer resources were provided by the Cy-Tera machine of CaSToRC, Forge at NCSA Illinois (USA), Minotauro at BSC (Spain), and Juqueen at the Jülich Supercomputing Center.

## References

- [1] A. Abdel-Rehim *et al.* (ETMC), Phys. Rev. **D89** (2014) 034501; C. Alexandrou *et al.* (ETMC), Comput.Phys.Commun. 185 (2014) 1370.
- [2] M. Clark, R. Babich, K. Barros, R. Brower, and C. Rebbi, Comp. Phys. Comm. **181** (2010) 1517; R. Babich, M. Clark, B. Joo, G. Shi, R. Brower *et al.*, arXiv:1109.2935.
- [3] A. Stathopoulos, J. Laeuchli, K. Orginos, (2013), arXiv:1302.4018.
- [4] M. Engelhardt *et al.*, PoSLaT**2014**, 139.
- [5] S. Bernardson, P. McCarty and C. Thron, Comp. Phys. Comm. **78** (1994) 256; K. Liu, Internal report UK/94-02, arXiv:hep-lat/09408007.
- [6] G. Bali, S. Collins and A. Schäffer, PoSLaT**2007** 141, arXiv:0709.3217; G. Bali, S. Collins and A. Schäffer, Comp. Phys. Comm.. **181** (2010) 1570.
- [7] C. Michael and C. Urbach (ETMC), PoSLaT**2007** 122, arXiv:0709.4564; P. Boucaud *et al.* (ETMC), Comp. Phys. Comm. **179** (2008), 695; S. Dinter *et al.* (ETMC), JHEP**1208** (2012), 037.
- [8] C. Alexandrou *et al.*, PoSLaT**2013** 411, arXiv:1401.6750
- [9] J.-W. Chen and M. Savage, Phys. Rev. **D66** (2002) 074509.
- [10] V. Drach, PhD dissertation; A. Ali Khan *et al.* (QCDSF-UKQCD), Nucl. Phys. **B689** (2004) 175; K. I. Ishikawa *et al.* (PACS-CS), arXiv:0905.0962.
- [11] C. Michael, M. S. Foster and C. McNeile (UKQCD), Nucl. Phys. **B83** (Proc. Suppl.) (2000) 185; A. O’Cais *et al.* (TrinLat), Comp. Phys. Comm. **172** (2005) 145; G. S. Bali, T. DÄijssel, T. Lippert, H. Neff and K. Schilling (SESAM), Phys. Rev. **D71** (2005) 114513.